Metal−Ligand Bonds of Second- and Third-Row d-Block Metals Characterized by Density Functional Theory

Kasper P. Jensen*

Department of Chemistry, Technical University of Denmark, DK-2800 Kongens Lyngby, Denmark

Received: June 30, 2009

This paper presents systematic data for 200 neutral diatomic molecules ML (M is a second- or third-row d-block metal and L = H, F, Cl, Br, I, C, N, O, S, or Se) computed with the density functionals TPSSh and BP86. With experimental structures and bond enthalpies available for many of these molecules, the computations first document the high accuracy of TPSSh, giving metal−ligand bond lengths with a mean absolute error of ∼0.01 Å for the second row and 0.03 Å for the third row. TPSSh provides metal−ligand bond enthalpies with mean absolute errors of 37 and 44 kJ/mol for the second- and third-row molecules, respectively. Pathological cases (e.g., HgC and HgN) have errors of up to 155 kJ/mol, more than thrice the mean (observed with both functionals). Importantly, the systematic error component is negligible as measured by a coefficient of the linear regression line of 0.99. Equally important, TPSSh provides uniform accuracy across all three rows of the d-block, which is unprecedented and due to the 10% exact exchange, which is close to optimal for the d-block as a whole. This work provides an accurate and systematic prediction of electronic ground-state spins, characteristic metal−ligand bond lengths, and bond enthalpies for many as yet uncharacterized diatomics, of interest to researchers in the field of second- and third-row d-block chemistry. We stress that the success of TPSSh cannot be naively extrapolated to other special situations such as, e.g., metal−metal bonds. The high accuracy of the procedure further implies that the effective core functions used to model relativistic effects are necessary and sufficient for obtaining accurate geometries and bond enthalpies of second- and third-row molecular systems.

Introduction

This paper reports accurate and systematic, computed bond lengths, bond enthalpies, and ground states for 200 neutral diatomics ML, where M is a second- or third-row d-block metal, and L is either H, F, Cl, Br, I, C, N, O, S, or Se. Metal−ligand bonds are of tremendous importance in catalysis, and the study of the essential units—the diatomics—is the first and foremost approach to obtaining much desired insight, as most trends carry on to more complex molecules.[1] The data presented here, which have not been obtained systematically before, neither by experimental methods nor by theoretical calculations, have negligible systematic errors and can serve as reference data for researchers working in the field of second- and third-row d-block chemistry.

It is well-accepted that density functional theory (DFT) today constitutes the most widely used theoretical method for describing electronic structure.[2] DFT can potentially describe any molecular system to any accuracy. Unfortunately, no universally applicable functional exists, since there is no simple analytical form that captures universally the connection between any electron density and its associated energy. Whereas ab initio studies of transition metal diatomics have been carried out in much detail,[3] also in more systematic ways,[4] the methods are far too time-consuming to be used in routine studies of larger molecular systems. Furthermore, imbalances in truncations of active spaces and one-electron spaces (basis sets) easily lead to unbalanced correlation of electrons, whereas DFT correlates all electrons consistently via the functional.

Despite the lack of universality, DFT has a hierarchy of accuracy just as ab initio methods: whereas the hierarchy in ab initio methods is determined by the complexity of the wave function, i.e., the sizes of the one- and many-electron spaces, in DFT it is Jacob's ladder[5,6] of physically justified, increased complexity of functionals, using one simple, effective determinantal wave function. Although this is not a variational procedure, it is stringent if the functional can be shown to provide systematically better energies without adding new parameters. Both paths can lead to any desired accuracy, but ab initio has traditionally been argued to be more stringent, due to the simple recipe for increased accuracy by expansion of the one- and many-electron spaces.

Thus, in principle, increased accuracy is achieved going from functionals that depend only locally on the density itself (local spin density approximations), to those that depend also on the gradient of the density (generalized gradient approximation, GGA), to those that furthermore depend on the kinetic energy density as well (meta functionals).[5,6] The additional incorporation of some amount of exact exchange (hybrid functionals) has been seen to enhance accuracy further:[7] The reason is related to the degree of electronic coupling (nondynamic correlation and nonlocality) in molecular systems, which is hard to achieve in any other simple analytical form than exact Hartree−Fock exchange.

With these tools, DFT has a systematic path toward higher accuracy. Following this path, it is absolutely necessary that new functionals are constantly tested against experimental data, in order to understand and improve them to the point where they can be used with confidence.[8]

* E-mail: kpj@kemi.dtu.dk.

10.1021/jp9061225 CCC: $40.75
Published on Web 08/14/2009

Most commonly used density functionals have been developed for the study of main group molecules.[9] The most widely used hybrid functional, B3LYP,[7] displays a mean absolute error of ca. 10 kJ/mol for enthalpies of formation, and 0.013 Å for bond distances for the main group G2 test set.[7] The amount of exact exchange was optimized to be ca. 20% for these benchmarks and included as a fixed parameter in the functional.[7] This success has made B3LYP the most widely used functional today, possibly even within the field of transition metal chemistry.[10]

However, when moving from main block elements to transition metals, electronic configurations come very close in energy and nondynamical correlation increases.[3] Certain insensitive properties, including bond lengths and vibration frequencies of strong bonds and isodesmic reaction energies, may still be modeled accurately with the most functionals[11,12] using hybrid[7] or nonhybrid functionals such as BP86[13,14] with equal success.[15]

Importantly, when nondynamical correlation changes substantially during a process, the often stated errors of ∼20 kJ/mol (∼5 kcal/mol)[12,16] are largely understated, which is seen as soon as one models, e.g., binding of ligands to metal centers,[10,17] homolytic cleavage of metal−ligand bonds,[18] one-electron transfer, and spin inversion.[17,19] All these processes depend on the treatment of exchange in DFT, and exact exchange favors the more open-shell electronic configurations.[18] This leads to an artificial bias of B3LYP toward high-spin configurations and dissociated states.[18−20] In some of these cases, nonhybrid functionals such as BP86 perform much better than hybrid functionals.[18,21,22]

Using GGA functionals such as BP86, PBE, BLYP, or hybrid functionals such as B3LYP or PBE0, the mean absolute errors in simple metal−ligand bond enthalpies are 43−52 kJ/mol with largest errors of more than 100 kJ/mol,[22] giving a more realistic account of the errors in modeling transition metal systems. Importantly, these errors are quite systematic and the energies are linearly dependent on the amount of exact exchange.[22]

As discussed early by Perdew et al.,[23] the amount of exact exchange to be incorporated in a functional depends on the coupling between electrons in the system of study, as given by the adiabatic connection formula.[24] Perturbation theory can be used to rationalize why 20−25% exact exchange, as seen in B3LYP and PBE0, performs well for main group elements.[23] Furthermore, it was suggested that near-degenerate ground states of the uncorrelated wave functions, i.e., states with a large component of nondynamical correlation, will require a smaller amount of exact exchange, sometimes giving better performance of nonhybrid functionals.[23] A version of B3LYP with 15% exact exchange performs better than B3LYP for iron(II) complexes,[25] and a version of BP86 with 10% exact exchange provides the best results for some FeNO and FeO_2 complexes,[26] illustrating this point.

The TPSSh meta hybrid functional[6,27] is nonempirical except for the $a = 0.1$ coefficient of exact exchange (10%), i.e., it does not rely on parameters as do other functionals such as B3LYP and BP86.[6] TPSSh generally performs similar to B3LYP for the G3/99 set[28] but outperforms both B3LYP and nonhybrid functionals in more general studies of first-row transition metal diatomics.[17,29]

For transition metal−metal bonds, the nonhybrid TPSS has been reported to perform best,[30] most likely because these systems embody strong nondynamical correlation, whereas other studies[31] document the large differences between hybrid and nonhybrid functionals and shortcomings in both: this is also true for second- and third-row d-block metal dimers.[32] Other benchmarks of transition metal systems with other functionals include studies of equilibrium geometries,[33] bond energies,[34] and excitation energies.[35]

In this work, we provide a new and systematic data set for the 200 possible diatomics composed from one metal of the second- and third-row d-block metals and either H, F, Cl, Br, I, C, N, O, S, or Se, computed with TPSSh. The data set consists of electronic ground states, bond lengths, and bond enthalpies and is envisioned to be helpful in future estimates of reactivity, in particular in the field of catalysis involving second- and third-row d-block metals.

Methods

Calculations were performed with the Turbomole 5.10 software.[36] The data consisted of all possible neutral diatomic molecules of Y−Cd in the first row and La−Hg in the third row, bound to H, F, Cl, Br, I, N, C, O, S, or Se, altogether 200 molecules.

The molecules were geometry-optimized in all relevant electronic configurations using a spin-down coupling procedure, to find the global minimum in each case: computation of configurations with lower M_S values can systematically be computed from higher M_S values, as the orbitals will tend to converge well from these.

Energies were converged down to 10^{-7} hartree, and the gradient was converged down to 10^{-3} au. Unrestricted calculations were performed in all cases, even where closed-shell configurations might be possible, to avoid singlet instabilities. This approach is more direct than attempting to compute closed-shell instabilities in individual cases and then probe for instabilities afterward.

The basis set used was def2-TZVP.[37] We have shown earlier[22] that a larger QZVPP basis set performs marginally better, giving a 1 kJ/mol smaller rms error for bond dissociation enthalpies (BDEs), consistent with consensus that basis set convergence is fast in DFT. Our applied basis set is probably larger than used in standard studies of larger systems of more limited scope. However, the aim of this work is not simply to probe typical accuracy in such modeling studies but also to use the high accuracy deduced here to predict properties de novo for many of these uncharacterized systems in their own right, to be used as a reference by other researchers. To this end, it was deemed necessary to use a triple-ζ basis set with diffuse and polarization functions.

For heavier metals, relativistic effects are of substantial importance and are known to have a substantial effect on the contraction of the core orbitals, expansion of the diffuse valence d-orbitals, and resulting metal-bond enthalpies. Therefore, all molecules have been treated consistently not only with such effective core potentials but also with correction for scalar-relativistic effects of the remaining outer electrons. As expected, the scalar-relativistic corrections are small for electrons outside the effective core, since most of the effects are already accounted for in the core potentials (see the Supporting Information, Tables S1−S3). However, for consistency, all energies reported here include also the scalar-relativistic corrections computed using Turbomole.

Effective 28-electron (for second row) and 60-electron (for third row) core potentials (def2-ecp) including scalar-relativistic effects were used for all metals.[38] A few test calculations with another effective core potential (sk-rsc-60-mdf) were also done on the gold molecules, which are considered to be particularly sensitive to relativistic effects. The results in Supporting Information Table S4 show that calculations are sensitive to

TABLE 1: TPSSh-Computed $2M_S + 1$ Followed by Experimental Ground States When Available[a]

	Y	Zr	Nb	Mo	Tc	Ru	Rh	Pd	Ag	Cd
H	1	4	5	6	5	4	3	2	1 $^1\Sigma^+$	2 $^2\Sigma^+$
F	1 $^1\Sigma^+$	2	5	6	5	4	3	2	1	2
Cl	1 $^1\Sigma^+$	2	5	6	5	4	3	2	1	2
Br	1	4	5	6	5	4	3	2	1	2
I	1	4	5	6	5	4	3	2	1 $^1\Sigma^+$	2
C	2	3	2	3	4	3	2	1	2	2
N	1	2	3	4	3	2	3	4	3	4
O	2 $^2\Sigma^+$	3 $^1\Sigma^+$ [b]	4 $^4\Sigma^-$	5	6	5	4	3	2 $^2\Pi_{1/2}$	1
S	2	1	4	5	6	5	4	1	2	1
Se	2	3	4	5	6	5	4	1	2	1

	La	Hf	Ta	W	Re	Os	Ir	Pt	Au	Hg
H	3	1	5	6	5	4	3	2 $^2\Delta_{5/2}$	1 $^1\Sigma^+$	2 $^2\Sigma^+$
F	3	2	3	6	5	4	3	2	1	2
Cl	1	2	5	6	5	6	3	2	1	2
Br	1	2	5	6	5	4	3	2	1	2
I	3	1	5	6	5	4	3	2	1	2
C	2	1	2	3	4	3 $^3\Sigma^-$ [c]	2	1 $^1\Sigma^+$	2	3
N	1	1	1	4	3	2	1	2	3	4
O	2 $^2\Sigma^+$	1	2 $^2\Delta_{3/2}$	3	4	5	4	3	2	3
S	2	1	4	5	6	5	2	3	2	1
Se	2	1	4	5	6	5	2	3	2	3

[a] Ref 39 except as noted in footnote. [b] Computed energy difference to singlet is 0.57 kJ/mol. [c] Ref 40.

the core potential, and using effective core potentials that are not optimized for a given system or basis set is dangerous. The accuracy of the calculations and the modest effects of scalar-relativistic effects beyond the core (Supporting Information Tables S1−S4) directly imply that relativistic effects are treated consistently and, thus, that such effective core functions are necessary and sufficient for producing accurate geometries and bond energies of second- and third-row molecular systems.

Frequencies were computed using the NumForce script. The BDEs were computed for all 200 molecules by computing the ground-state energies of the corresponding atoms and subtracting the ground-state energy of the geometry-optimized diatomic molecule. Zero-point energies (ZPE) and enthalpy corrections were calculated from subsequent harmonic frequency analysis and added to the energies to obtain bond enthalpies at standard conditions, for comparison with experimental data. The experimental data are from gas-phase experiments,[39] and thus, our calculations have not been corrected for medium effects.

Results and Discussion

Prediction of Electronic Ground States. We first evaluate the ability of TPSSh to obtain electronic ground states with spin quantum numbers consistent with experimental data. Obtaining the qualitatively correct electronic structure is the first obstacle to accurate predictions of molecular properties. In the computations, specific M_S values are used as constraints in separate optimization procedures. The electronic configuration with the lowest energy is considered the DFT approximation to the true ground state, and its associated M_S value is compared to the experimentally determined spin of the ground state to provide a first test of the quality of the computed electronic structure.

Table 1 displays the experimentally determined[39,40] state where known to the right of each entry and the computed value of $2M_S + 1$ for the configuration of lowest energy to the left. Only a few (16 identified at the time of producing this work) electronic ground states have been characterized under the standard conditions modeled here.[39,41]

As seen from Table 1, 15 of the 16 computed ground states exhibit M_S values consistent with experimental data, which parallels the average performance for other previously tested functionals.[22] The only case where an inconsistent M_S value is obtained, ZrO, displays almost degenerate electronic configurations for $M_S = 0$ and $M_S = 1$, with an energy difference of only 0.57 kJ/mol.

Therefore, there is a clear tendency for the computed electronic structures to be consistent with experimentally determined ground states. In the many cases where experimental data are not available, the computed ground states thus provide good approximations to the true ground states, with an estimated +90% confidence for this type of molecular system. However, given the scarce experimental data, this first test is not very strict, and it will be supplemented in the next sections by tests against experimental bond lengths and bond enthalpies.

Importantly, the BP86 functional gave the same results as TPSSh for these 16 molecules, even for ZrO, where in principle a bias toward the lower spin state would be anticipated due to the absence of exact exchange. As was seen in earlier work on first-row d-block diatomics,[17,22] most modern functionals will provide a good prediction of the real spin state, whereas the energy difference between states vary substantially. Importantly, in larger, more coordinatively saturated metal complexes, the energy differences between configurations become even smaller and accuracy will decrease, implying that prediction of ground-state spin by any DFT method is not necessarily good in larger molecules.

The metal spin populations for all 200 ground states have been computed using Mulliken population analysis and are visualized in Figure 1. The spin population on the metal dominates the total spin population and is clearly proportional to the M_S quantum number of the ground state. For many of these states, experimental data are as mentioned not available, so Figure 1 can be used to predict ground-state spins with high confidence where data are not available. The trend across the d-blocks quantifies the anticipation that the largest spin is found in the middle of the d-block, in particular for Mo and W, and that lower spin is found gradually going to either left or right. This observation is particular true for the halides and is due to the dominating M^+X^- configurations, which have five d-electrons in Mo and W. Spin coupling in the later metals or less d-electrons in the earlier metals lead to smaller spins. The tendency is less pronounced in the chalcogenides S and Se, and O, and even less in the carbides and nitrides, due to the involvement of other electronic configurations than M^+X^-.

Equilibrium Geometries. We now turn to the computed metal−ligand bond lengths, which are key benchmarks for computational predictions of structures of larger molecular systems: to model reactivity where bonds break or form, it is essential that these bonds are modeled accurately, and if this is not the case, it will manifest itself already in poor geometries. However, as has been shown,[22] accurate geometries are necessary but not sufficient for obtaining accurate chemical energies, since the nuclear positions are largely determined by the entire (nonvalence dominated) electron density, of which the correlated electron density is a small fraction, and thus the geometry is relatively insensitive in most cases to the electron correlation treatment, and many theoretical methods provide decent geometries.[22] However, when computing chemical energies, the exchange-correlation potential directly affects the valence electrons that mainly change during the process, and very different results are obtained with different theoretical methods.

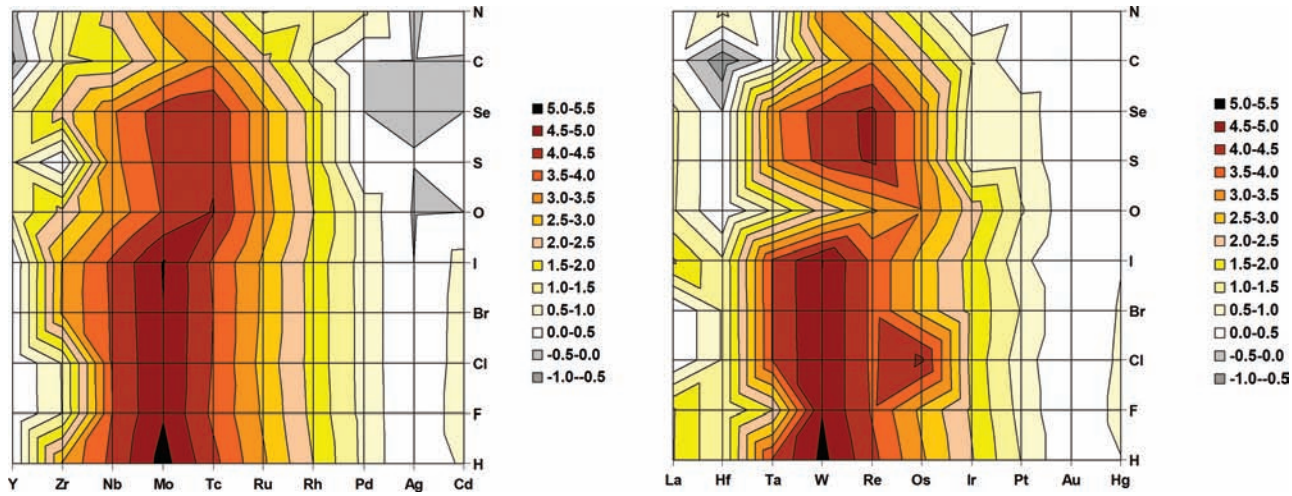

Figure 1. Computed spin populations on metals in diatomic molecules: comparison of second-row (left) and third-row (right) d-block.

The TPSSh-optimized equilibrium bond lengths are presented in Table 2. For each molecule, the experimental bond length,[39,41,42] when available, is listed above, and the computed bond length is below. The mean absolute errors (MAE) and largest absolute errors (LAE) are provided for each type of atom, to identify any particular trends in the performance of the functional with respect to element.

For the complete sets, the MAEs in computed bond lengths are 0.01 Å for the second-row molecules and 0.03 Å for the third-row molecules. The largest errors are seen in the bromides, iodides, and in the early part of the d-block, in particular La, Hf, and Zr. The largest error found for the second-row d-block is 0.03 Å, seen in ZrO and AgI. For ZrO, the computed bond length is 1.73 Å for the low-spin state and 1.74 Å for the computed high-spin ground state. Given that the experimentally determined state is low spin and has a bond length of 1.71 Å, this is reasonable. The largest error found for the third-row d-block is 0.10 Å, seen in HfH and LaBr. The reasons for the larger errors are most likely the covalency effects of the larger ligands and the electron correlation due to partial occupation of 5s and 6s orbitals in the metals. Future improvements based on TPSSh may focus on these aspects although it is clear that the amount of exact exchange appears to be near-optimal (vide infra).

The numbers in Table 2 confirm results from earlier studies,[17,29] showing that the TPSSh functional models the metal−ligand bond lengths as accurately as any other functional. As seen before, both GGA nonhybrid functionals such as BP86 and the 10% exact exchange hybrid TPSSh provide accurate geometries for metal complexes using this type of test,[17] which is due to the fact that metal−ligand bonds of this type are usually fairly strong and thus display little variation due to changes in functional.

The data in Table 2 can, given the accuracy deduced here, be used as a reference for "characteristic metal−ligand bond lengths" not presented before. Such characteristic bond lengths are useful as accurate descriptors of each type of chemical bond. Given the novelty of these data, some space is devoted on the next pages to compare important trends in the numbers.

The accuracies of the fundamental diatomics studied here are similar to those obtained for larger, coordinatively saturated second- and third-row transition metal complexes:[43,44] This implies that the accuracies observed for transition metal geometries are generally quite good, both when considering the full d-block systematically and when considering larger systems. Specifically, both these types of studies point toward DFT as a most accurate tool for describing geometries. TPSSh was seen in these studies to provide accurate geometries in these cases as well, although some nonmeta hybrid functionals displayed slightly better overall accuracy. It is thus reasonable to conclude that geometries are well-modeled by standard functionals and that problems mainly arise when modeling chemical energies. Such energies, in particular the bond enthalpies, are the main concern of this work.

One immediate observation from Table 2 is the contraction in metal−ligand bond lengths going from Y/La and to Rh/Ir, followed by expansion from Rh/Ir to Cd/Hg. This trend correlates with the successive occupation of diffuse d-orbitals, leading to a gradual decrease in the radius of the metal and a corresponding shortening of the metal−ligand bond lengths, followed by full occupation of the d-shell and, consequently, promotion to antibonding orbitals, which drastically increase the bond lengths after Rh/Ir.

The computed contraction, averaged over all 10 molecules of each metal, is depicted for the second and third row separately in Figure 2. Due to the scarcity of experimental data, only a few points on each line are known from experiments, and the computations can thus fill out the many missing points with MAE of 0.01−0.03 Å, but with some anticipated larger errors.

Bond Dissociation Enthalpies. The bond dissociation enthalpies are defined as the enthalpy of the two radical fragments (in this case atoms) minus the enthalpy of the complex, calculated for the ground states at standard conditions (1 atm and 298 K). The calculation details were discussed in the Methods section. These numbers are critical in modeling studies, since bond formation and bond breaking are at the heart of most relevant chemical processes. Unfortunately, the literature is full of molecular modeling studies where DFT has been used to deduce reactivity with a confidence that is not justified by the actual MAEs of the used functionals. This is true in most theoretical estimations of energy differences between structures differing qualitatively in electronic structure, including also the vast amount of studies relying on computed activation barriers, based on the assumption that the partially broken metal−ligand bonds in the transition state are accurately modeled by the density functional. The present paper represents part of a continued effort to convince the community that such barriers and energies have errors of easily 100 kJ/mol and that only a few functionals, viz. TPSSh, provide a reasonably accurate account of such processes.

TABLE 2: Experimental Bond Lengths (Top, Italics) Compared to TPSSh-Computed Bond Lengths (Bottom) (angstroms)[a]

	Y	Zr	Nb	Mo	Tc	Ru	Rh	Pd	Ag	Cd	MAE	LAE
H									*1.62*	*1.78*	0.00	0.00
	1.92	1.87	1.78	1.71	1.65	1.60	1.56	1.54	1.62	1.78		
F	*1.93*									*1.98*	0.01	0.01
	1.94	1.87	1.88	1.89	1.85	1.90	1.91	1.92	1.99	2.01		
Cl	*2.41*									*2.28*	0.01	0.01
	2.40	2.30	2.27	2.29	2.27	2.22	2.22	2.24	2.29	2.38		
Br										*2.39*	0.02	0.02
	2.55	2.49	2.45	2.44	2.41	2.35	2.33	2.37	2.41	2.52		
I									*2.54*		0.03	0.03
	2.79	2.73	2.65	2.63	2.54	2.55	2.56	2.53	2.57	2.72		
C				*1.68*		*1.61*	*1.61*	*1.71*			0.01	0.01
	2.05	1.80	1.71	1.67	1.65	1.62	1.61	1.71	2.01	2.18		
N												
	1.82	1.70	1.66	1.63	1.59	1.56	1.63	1.80	2.02	2.33		
O	*1.79*	*1.71*	*1.69*						*2.00*		0.01	0.03
	1.80	1.74	1.69	1.70	1.72	1.70	1.70	1.81	1.99	2.11		
S							*2.06*				0.00	0.00
	2.28	2.20	2.13	2.13	2.12	2.08	2.06	2.10	2.29	2.24		
Se												
	2.42	2.33	2.25	2.25	2.26	2.22	2.22	2.23	2.40	2.36		
MAE	0.01	0.03	0.00	0.01		0.01	0.00	0.00	0.01	0.00	0.01	
LAE	0.01	0.03	0.00	0.01		0.01	0.00	0.00	0.03	0.00		

	La	Hf	Ta	W	Re	Os	Ir	Pt	Au	Hg	MAE	LAE
H		*1.74*						*1.53*		*1.77*	0.04	0.10
	2.11	1.84	1.78	1.72	1.64	1.62	1.56	1.53	1.55	1.79		
F		*1.86*									0.01	0.01
	2.10	1.87	1.87	1.90	1.88	1.82	1.82	1.88	1.94	2.07		
Cl												
	2.58	2.31	2.30	2.28	2.22	2.15	2.17	2.16	2.23	2.42		
Br	*2.65*										0.10	0.10
	2.75	2.47	2.46	2.43	2.36	2.29	2.30	2.29	2.35	2.57		
I	*2.88*										0.08	0.08
	2.96	2.70	2.66	2.62	2.55	2.47	2.47	2.43	2.51	2.77		
C				*1.71*				*1.68*			0.01	0.01
	2.01	1.81	1.77	1.72	1.70	1.67	1.68	1.68	1.87	2.16		
N								*1.68*			0.01	0.01
	1.89	1.74	1.70	1.67	1.64	1.61	1.60	1.69	1.89	3.52		
O	*1.83*		*1.69*					*1.73*			0.03	0.09
	1.92	1.73	1.69	1.66	1.74	1.72	1.73	1.73	1.89	2.20		
S									*2.04*		0.01	0.01
	2.41	2.33	2.15	2.14	2.14	2.09	2.06	2.05	2.20	2.54		
Se												
	2.55	2.31	2.28	2.28	2.27	2.22	2.19	2.18	2.32	2.68		
MAE	0.09	0.06		0.01				0.01		0.02	0.03	
LAE	0.10	0.10		0.01				0.01		0.02		

[a] Refs 39 and 41. MAE: mean absolute error. LAE: largest absolute error.

Table 3 shows the experimentally determined BDEs.[39,41] A total of 45 and 37 experimental values have been identified, giving a total of 82 data points. Few data points are available for the bromides, iodides, nitrides, Tc, and Re, and many for oxides, and early and late d-block metals. However, there is overall a comfortable spread in experimental numbers, which allows us to validate accuracy broadly across the d-block.

Already from the experimental data in Table 3, it can be seen that bond enthalpies decrease going from left to right in the d-block (the most important exception being the carbides). As the d-orbitals are occupied, the bond lengths contract, and one would anticipate stronger bonds going from Y/La toward Rh/Ir, consistent with the metal−ligand bond lengths. Such an inverse correlation between bond length and bond enthalpy is observed only at the very right side of the d-block, i.e., in Pd, Ag, and Cd.

The reason for the lack of correlation in the remaining part of the d-block is the fact that the dissociated atomic states play

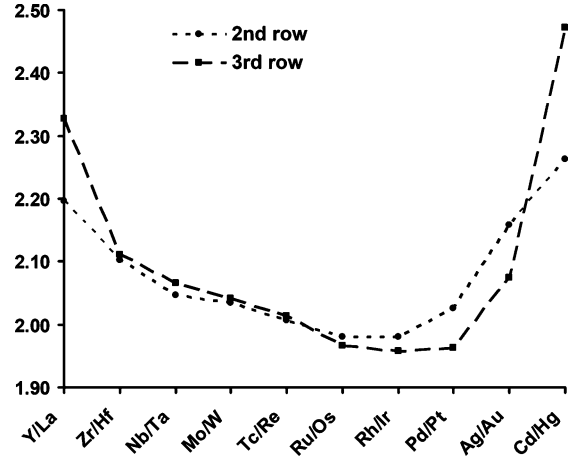

Figure 2. TPSSh-computed trends in average metal−ligand bond lengths.

TABLE 3: Experimental Bond Dissociation Energies (kJ/mol)[a]

	Y	Zr	Nb	Mo	Tc	Ru	Rh	Pd	Ag	Cd
H						234	247	234	215	69
F	605	616		465		402			354	305
Cl	527								341	208
Br	485								293	159
I		305							234	97
C	418	561	569	481	565	616	580			
N	481	565								
O	720	776	772	560		528	405	381	220	236
S	528	575							217	208
Se	435								203	128

	La	Hf	Ta	W	Re	Os	Ir	Pt	Au	Hg
H								335	292	40
F	598	650	573	548						180
Cl			544	423					343	100
Br				329						73
I										35
C		540				594	632	598		
N		536	611							
O	678	802	799	672	627	575	415	392	222	221
S	507								418	217
Se	418								243	144

[a] Refs 39 and 41.

an equally important role in determining the total bond enthalpy. In particular, the free metal atoms experience an equal stabilization due to d-orbital contraction as seen in the diatomic molecules.

Table 4 displays the deviations between experimental and TPSSh-computed bond enthalpies and the corresponding MAEs for each class of molecules. A positive number implies that the experimental bond enthalpy is larger than the computed bond enthalpy.

Overall, the TPSSh functional performs almost as well for second- and third-row diatomics as it does for first-row diatomics:[17] The overall MAEs of 37 kJ/mol for the second row and 44 kJ/mol for the third row are contrasted by an MAE of 34 kJ/mol for the first row of the d-block. A spread in MAEs of 10 kJ/mol, or only ~25% across the three rows, is remarkable and unprecedented by any method. This illustrates that TPSSh performs uniformly well across all three rows, which is extremely important when devising a method that can compare trends in modeled complexes across the entire d-block.

Larger than expected errors are found in the iodides, and in Cd and Hg, which is due to the size of iodine and the complex electron correlation arising from occupation of the 5s and 6s orbitals in these metals. As seen in Supporting Information (Table S1), the neglect of scalar-relativistic effects outside the 18-electron effective relativistic core has very limited negative effect on the overall MAEs but increases the systematic error component from an average of −5 and 2 kJ/mol per molecule to 11 and 14 kJ/mol, respectively, for the second- and third-row molecules. In the second row, the carbides of Pd and Cd have LAEs of 84 and 103 kJ/mol. For the third row, HgC and HgN have the largest errors (155 and 146 kJ/mol), which are 3 times larger than the total MAE and indicate pathological cases. These compounds may require further studies, in particular using multiconfigurational methods.

In earlier work on the first row of the d-block, other functionals were tested, and the result was that TPSSh performs better than any nonhybrid GGA functional or any hybrid with 20% exact exchange or more (B3LYP, PBE0), with MAEs between 46 and 57 kJ/mol.[17,22] It was found that many energies (ionization potentials, spin inversion, metal−ligand bond breaking) are linearly related to the amount of exact exchange included in the functional and thus that TPSSh eliminates a large systematic error component of other functionals.[17] In addition, TPSSh is nonempirical except for the 10% exact exchange,[28] which can be partly rationalized as described in the Introduction.[23]

TABLE 4: Errors in Computed Bond Dissociation Enthalpies, Including Zero-Point Energies, Scalar-Relativistic Corrections, and Thermal Corrections (kJ/mol)[a]

	Y	Zr	Nb	Mo	Tc	Ru	Rh	Pd	Ag	Cd	MAE	LAE
H						−51	−62	−50	−47	−59	54	62
F	−57	−23		−14		−7			5	30	23	57
Cl	12								10	−19	14	19
Br	31								−16	−41	29	41
I		−71							−52	−70	64	71
C	25	5	38	38		41	−9	84	−1	103	38	103
N	−12	−11							−36	67	31	67
O	−52								−39	−1	30	52
S	59	63	65	18	−59	10	7				40	65
Se	71	−25									48	71
MAE	40	33	51	24	59	27	26	67	26	49	37	
LAE	71	71	65	38	59	51	62	84	52	103		

	La	Hf	Ta	W	Re	Os	Ir	Pt	Au	Hg	MAE	LAE
H								−22	−25	−42	30	42
F	−34	−21	−5	32						10	20	34
Cl			102	11					42	−35	47	102
Br				−36						−42	39	42
I										−58	58	58
C	−19	−1	30	26	118	54	−62	−32	−11	155	51	155
N	−46									146	96	146
O	−86								−18	80	61	86
S		92				−59	−4	−21			44	92
Se		−6	6								6	6
MAE	46	30	36	26	118	56	33	25	24	71	44	
LAE	86	92	102	36	118	59	62	32	42	155		

[a] TPSSh functional.

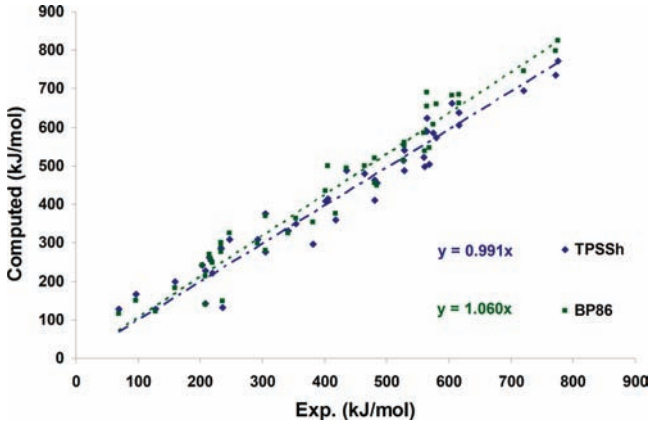

Figure 3. Computed vs experimental metal−ligand bond enthalpies for the second-row d-block.

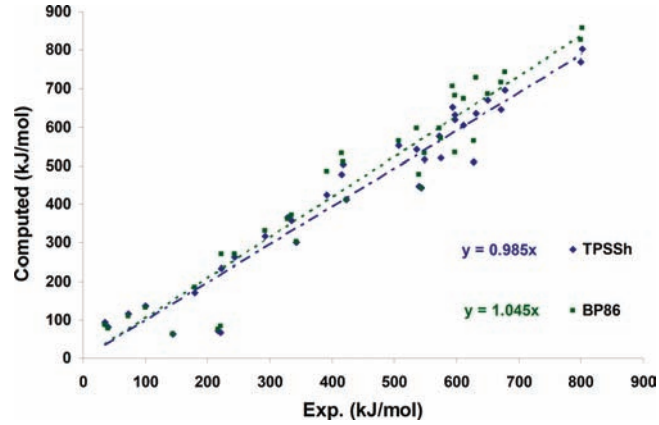

Figure 4. Computed vs experimental metal−ligand bond enthalpies for the third-row d-block.

In comparison to previous studies of metal−metal dimer bond dissociation energies studied with the BOP and B3LYP functionals,[32] the present TPSSh calculations perform substantially better even in absolute numbers: For BOP, MAEs were 63, 53, and 19 kJ/mol for first-, second-, and third-row transition metal dimers, whereas for B3LYP, MAEs were 67, 62, and 37 kJ/mol. Given that the bond dissociation energies in dimers are numerically smaller by several hundred kilojoules per mole, the errors are even larger percentwise. This is most likely due to the complex electron correlation effects found in the metal−metal bonds, which are beyond the scope of this work.

In order to put the results into perspective with ab initio data, the TPSSh results have been compared to specific results obtained from earlier CI-based ab initio studies.[1,3,4] Comparison is not straightforward, since the present data sets are much more extensive, and include the difficult early and late metals as well. However, we can compare earlier computed[4] second-row d-block (Y−Pd) hydrides, fluorides, and chlorides, with our results. Summed over nine numbers where experimental data are available, the ab initio computations give an MAE of 27.7 kJ/mol, where TPSSh gives 34.5 kJ/mol. Given that ab initio methods cannot routinely be performed for larger molecular systems, whereas TPSSh can, this is encouraging.

In contrast to hybrid functionals with 20% or more exact exchange (B3LYP, PBE0), the GGA nonhybrid functionals are anticipated to perform well for the later rows of the d-block due to stronger nondynamical correlation,[17,23] and it is relevant to observe the performance of such a functional, to validate the accuracy of TPSSh for computing new reference data.

To this end, we have geometry-optimized the 200 diatomics also with the BP86 functional and computed the corresponding free atom energies, all using the same methodology as for TPSSh. The data, found in the Supporting Information (Table S3), show that BP86 performs well for the second row, with an MAE of 44 kJ/mol, but not so well for the third row, with an MAE of 58 kJ/mol. This is initially surprising, as less exact exchange would be anticipated to be more accurate later in the periodic table due to increased nondynamical correlation. The introduction of scalar-relativistic effects (Supporting Information Table S2) makes the performance of BP86 worse: had one neglected these, MAEs would have been 39 and 53 kJ/mol, respectively. However, still without relativistic effects, TPSSh is more accurate, as evident from the computed MAEs.

The performance of the two functionals is summarized graphically in Figures 3 (second row) and 4 (third row). The linear correlation between experimental and theoretical metal−ligand bond enthalpies directly reveals systematic errors. For the second row (Figure 3), TPSSh has a coefficient of the linear correlation line of 0.991, whereas that of BP86 is 1.060. This implies, as also observed for the first-row d-block,[17,22] that BP86 (as other nonhybrid GGA functionals) overestimates the bond enthalpy and bond strengths in a general way, whereas the systematic error component of TPSSh is significantly smaller than for other theoretical methods. For the third row (Figure 4) the advantage of TPSSh over BP86 is slightly less pronounced, but still comparable to the situation in the second row, with coefficients of 0.985 and 1.045, respectively, from TPSSh and BP86. Although an actual benchmark study of functionals is beyond the scope of this work, the comparison of TPSSh and BP86 does provide us with further confidence that our computed reference data for the 200 molecules are of the stated accuracy and thus of substantial interest to researchers in the field.

TABLE 5: Computed Bond Dissociation Enthalpies, Including Zero-Point Energies, Scalar-Relativistic Corrections, and Thermal Corrections (kJ/mol)[a]

	Y	Zr	Nb	Mo	Tc	Ru	Rh	Pd	Ag	Cd
H	290	307	288	149	276	285	309	284	262	128
F	662	639	573	479	454	409	390	363	349	275
Cl	515	484	396	385	369	357	333	327	331	227
Br	454	428	402	341	332	324	325	298	309	200
I	393	376	346	294	306	294	300	270	286	167
C	359	498	504	463	624	606	573	374	194	141
N	410	590	597	518	527	452	349	260	158	59
O	695	771	734	522	556	487	414	297	221	133
S	540	586	541	388	471	418	370	304	253	141
Se	487	526	437	252	423	372	332	281	242	129
	La	Hf	Ta	W	Re	Os	Ir	Pt	Au	Hg
H	281	293	284	297	242	280	340	357	317	82
F	632	671	578	516	354	426	359	350	304	170
Cl	499	501	442	412	254	358	355	342	301	135
Br	451	442	391	365	207	317	323	318	283	115
I	393	369	332	314	159	279	297	304	270	93
C	424	448	510	482	573	653	636	619	311	107
N	483	542	605	587	515	554	516	375	216	29
O	697	803	769	646	509	521	477	424	233	66
S	553	566	556	453	413	444	398	437	276	71
Se	504	526	493	395	361	393	362	401	261	64

[a] TPSSh functional.

After having established the accuracy of the procedure, we now discuss in more detail the TPSSh-computed metal−ligand bond enthalpies, compiled in Table 5. In order to analyze these results, a graphical landscape of metal−ligand bond enthalpies can be produced, as shown in Figure 5. This type of descriptor landscape can be used in computational modeling for fast

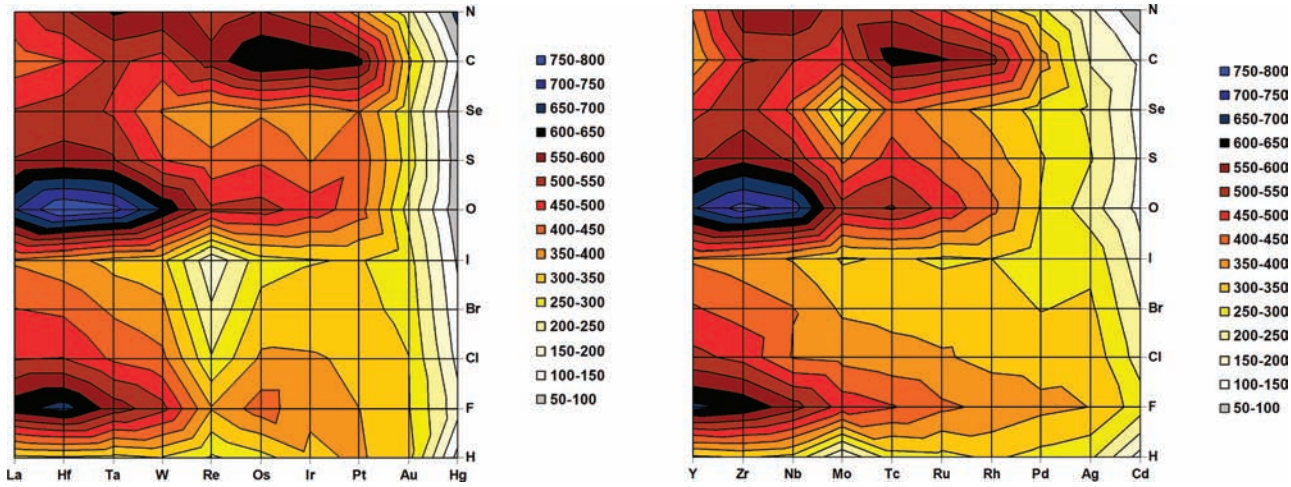

Figure 5. TPSSh-computed bond enthalpies: comparison of second-row (left) and third-row (right) d-block.

screening of properties, e.g., in the search for potential new catalytic systems. The computed bond enthalpies in Table 5 and Figure 5 also reveal interesting similarities and differences between the second-row and third-row d-blocks. Given that the experimental data are not available to generate these landscapes, this is an example of the benefit of using computational chemistry for understanding molecular structure and stability.

A main observation from Figure 5 is the similar positions of "mountains" in both landscapes: The strongest bonds are found in the early metal oxides, the early fluorides, and the late-middle carbides. This tendency is confirmed by those experimental data available, but the picture is more complete in Figure 5. The heavier halides display the smallest differences in bond strength across the rows, whereas fluorides and oxides change dramatically across the rows.

It can be seen that the inclusion of relativistic effects via the effective core potentials (def2-ecp) leads to a consistent treatment of geometries and bond enthalpies, regardless of the size of the metal. This, together with the uniform performance of TPSSh in terms of nondynamic correlation, is key to overall uniform accuracy when going from the second row to the third row of the d-block. It is worth mentioning that effective core potentials were not used in the previous studies of the first-row d-block,[17,22] where similar accuracy was obtained, so in the present scheme aimed at obtaining uniform accuracy across the entire d-block, it is necessary to include effective core potentials in the second and third rows only, to achieve uniform accuracy. The scalar-relativistic corrections for the valence electrons are small and not absolutely necessary in full-scale modeling studies. The effective core potentials used in going from second to third row have not lowered errors significantly, implying a consistent treatment of relativity.

The oxophilicity of metals is often quantified from the ability to form oxides and correlates with the Lewis acid strength of the metal. It can be seen from Table 5 and Figure 5 that the computed bond enthalpies correlate well with this concept of oxophilicity, and the computed metal−oxo bond enthalpies provide a useful definition of oxophilicity for direct comparison between all metals.

In what we refer to as "computational-chemical evolution",[45] new molecular clusters are screened for optimal descriptors in chemical landscapes such as Figure 5. One such descriptor will often be the strength of a metal−ligand bond, of crucial importance in catalytic studies. It is known that these bond strengths are difficult to model due to the presence of differential correlation effects,[17,22] and many theoretical methods, including various density functionals, exhibit largest errors well above 100 kJ/mol and MAEs of 50 kJ/mol or more. In the search for an optimal metal−ligand bond, strong enough to prevail until reaction but weak enough to break during reaction, using B3LYP or pure GGA functionals will propagate errors since the rate-limiting catalytic step usually does not benefit from cancellation of errors: It will usually be, e.g., a bond-breaking or bond-forming step. For these reasons, extreme care must be exercised when using theoretical methods to estimate descriptors. This work shows that TPSSh is a most viable method for describing second- and third-row d-block chemistry at high computational speed. However, this success is *not* to be assumed transferable to special situations such as, e.g., metal−metal bonds. The data presented in here, the metal−ligand bond lengths and bond enthalpies, can serve as reference data in future estimates, useful in many areas of catalysis.

In conclusion, in previous work,[17] we have identified a strong linear correlation between the amount of Hartree−Fock exchange in a functional and the computed reaction energies for a variety of the most relevant chemical reaction types, including bond dissociations, reductions, and spin inversions: 10% Hartree−Fock exchange in a hybrid was found to be optimal for the first row of the d-block, whereas B3LYP and BP86, respectively, under- and overestimate bond energies due to their bias toward atomic and molecular states, respectively.[17] The importance of balancing the electron correlation effects, in particular the Fermi correlation, on both sides of the equation of these chemical processes has been emphasized.

Here, by studying a data set of 200 diatomics with one metal of the second- or third-row d-block, we find that 10% Hartree−Fock exchange retains a negligible systematic error, as seen in a 0.99 coefficient for a linear correlation line between computed and experimental bond enthalpies. The absence of a systematic error component and uniform accuracy with MAEs of 35−45 kJ/mol across the entire d-block suggest that electron correlation can be treated in a balanced manner for the d-block as a whole; this is exceedingly important when modeling chemistry across the rows. In the outlined computational procedure, one should use TPSSh without effective core potentials for the first-row d-block and with 18-electron and 40-electron effective relativistic core potentials for the second- and third-row of the d-block, respectively.

Acknowledgment. The Danish Center for Scientific Computing (DCSC) and the Danish National Science Research Council (FNU) are gratefully acknowledged for supporting this work.

Supporting Information Available: Computed metal−ligand bond enthalpies without relativistic corrections using TPSSh (Table S1), without relativistic corrections using BP86 (Table S2), and with relativistic corrections using BP86 (Table S3), and the effect of using a larger effective core potential on the computed bond dissociation enthalpies (Table S4). This material is available free of charge via the Internet at http://pubs.acs.org.

References and Notes

(1) Langhoff, S. R.; Pettersson, L. G. M.; Bauschlicher, C. W., Jr.; Partridge, H. *J. Chem. Phys.* **1991**, *86*, 268–278.
(2) Geerlings, P.; De Proft, F.; Langenaeker, W. *Chem. Rev.* **2003**, *103*, 1793–1873.
(3) Langhoff, S. R.; Bauschlicher, C. W., Jr. *Annu. Rev. Phys. Chem.* **1988**, *39*, 181–212.
(4) Siegbahn, P. E. M. *Theor. Chim. Acta* **1993**, *86*, 219–228.
(5) Perdew, J. P.; Kurth, S.; Zupan, A.; Blaha, P. *Phys. Rev. Lett.* **1999**, *82*, 2544–2547.
(6) Tao, J.; Perdew, J. P.; Staroverov, V. N.; Scuseria, G. E. *Phys. Rev. Lett.* **2003**, *91*, 146401.
(7) Becke, A. D. *J. Chem. Phys.* **1993**, *98*, 5648–5652.
(8) Zhao, Y.; Truhlar, D. G. *Acc. Chem. Res.* **2008**, *41*, 157–167.
(9) Bauschlicher, C. W. *Chem. Phys. Lett.* **1996**, *246*, 40–44.
(10) Siegbahn, P. E. M. *J. Biol. Inorg. Chem.* **2006**, *11*, 695–701.
(11) Frenking, G.; Frohlich, N. *Chem. Rev.* **2000**, *100*, 717–774.
(12) Siegbahn, P. E. M.; Blomberg, M. R. A. *Chem. Rev.* **2000**, *100*, 421–437.
(13) Becke, A. D. *Phys. Rev. A* **1988**, *38*, 3098–3100.
(14) Perdew, J. P. *Phys. Rev. B* **1986**, *33*, 8822–8824.
(15) Ziegler, T. *Chem. Rev.* **1991**, *91*, 651–667.
(16) Blomberg, M. R. A.; Siegbahn, P. E. M.; Svensson, M. *J. Chem. Phys.* **1996**, *104*, 9546–9554.
(17) Jensen, K. P. *Inorg. Chem.* **2008**, *47*, 10357–10365.
(18) Jensen, K. P.; Ryde, U. *J. Phys. Chem. A* **2003**, *107*, 7539–7545.
(19) Neese, F. *J. Biol. Inorg. Chem.* **2006**, *11*, 702–711.
(20) Zein, S.; Borshch, S. A.; Fleurat-Lessard, P.; Casida, M. E.; Chermette, H. *J. Chem. Phys.* **2007**, *126*, 014105.
(21) Li, J.; Schreckenbach, G.; Ziegler, T. *J. Am. Chem. Soc.* **1995**, *117*, 486–494.
(22) Jensen, K. P.; Roos, B. O.; Ryde, U. *J. Chem. Phys.* **2007**, *126*, 014103.
(23) Perdew, J. P.; Ernzerhof, M.; Burke, K. *J. Chem. Phys.* **1996**, *105*, 9982–9985.
(24) Harris, J.; Jones, R. O. *J. Phys. F: Met. Phys.* **1974**, *4*, 1170–1186.
(25) Reiher, M. *Inorg. Chem.* **2002**, *41*, 6928–6935.
(26) Schenk, G.; Pau, M. Y. M.; Solomon, E. I. *J. Am. Chem. Soc.* **2004**, *126*, 505–515.
(27) Perdew, J. P.; Tao, J.; Staroverov, V. N.; Scuseria, G. E. *J. Chem. Phys.* **2004**, *120*, 6898–6911.
(28) Staroverov, V. N.; Scuseria, G. E.; Tao, J.; Perdew, J. P. *J. Chem. Phys.* **2003**, *119*, 12129–12137.
(29) Furche, F.; Perdew, J. P. *J. Chem. Phys.* **2006**, *124*, 044103.
(30) Zhao, Y.; Truhlar, D. G. *J. Chem. Phys.* **2006**, *124*, 224105.
(31) Barden, C. J.; Rienstra-Kiracofe, J. C.; Schaefer, H. F., III. *J. Chem. Phys.* **2000**, *113*, 690–700.
(32) Yanagisawa, S.; Tsuneda, T.; Hirao, K. *J. Comput. Chem.* **2001**, *22*, 1995–2009.
(33) Buhl, M.; Kabrede, H. *J. Chem. Theory Comput.* **2006**, *2*, 1282–1290.
(34) Schultz, N. E.; Zhao, Y.; Truhlar, D. G. *J. Phys. Chem.* **2005**, *109*, 11127–11143.
(35) Holthausen, M. C. *J. Comput. Chem.* **2005**, *26*, 1505–1518.
(36) Ahlrichs, R.; Bär, M.; Häser, M.; Horn, H.; Kölmel, C. *Chem. Phys. Lett.* **1989**, *162*, 165–169.
(37) Weigend, F.; Ahlrichs, R. *Phys. Chem. Chem. Phys.* **2005**, *7*, 3297–3305.
(38) Andrae, D.; Haussermann, U.; Dolg, M.; Stoll, H.; Preuss, H. *Theor. Chim. Acta* **1990**, *77*, 123–141.
(39) Lide, D. R., Ed. *Handbook of Chemistry and Physics*, 87th ed.; CRC Press: Boca Raton, FL, 2006−2007.
(40) Meloni, G.; Thomson, L. M.; Gingerich, K. A. *J. Chem. Phys.* **2001**, *115*, 4496.
(41) Boldyrev, A.; Simons, J. *Periodic Table of Diatomic Molecules*; John Wiley & Sons: New York, 1997 (ISBN: 0471965154).
(42) Barnes, M.; Merer, A. J.; Metha, G. F. *J. Chem. Phys.* **1995**, *103*, 8360–8371.
(43) Waller, M. P.; Braun, H.; Hojdis, N.; Buhl, M. *J. Chem. Theory Comput.* **2007**, *3*, 2234–2242.
(44) Buhl, M.; Reimann, C.; Pantazis, D. A.; Bredow, T.; Neese, F. *J. Chem. Theory Comput.* **2008**, *4*, 1449–1459.
(45) Jensen, K. P. In *Encyclopedia of Inorganic Chemistry: Computational Inorganic and Bioinorganic Chemistry*; Solomon, E. I., Scott, R. A., King, R. B., Eds.; in press.

JP9061225